The Impact of Damping on the Frequency Stability of Nonlinear MEMS Oscillators

Xudong Zou, *Member, IEEE*, Ashwin A. Seshia, *Senior Member, IEEE*

***Abstract*— Linear models for oscillator noise predict an improvement in frequency stability with increasing Quality factor. Although it is well known that this result does not apply to non-linear oscillators, systematic experimental investigations of the impact of damping on frequency stability of non-linear MEMS oscillators has not been previously reported. This paper studies the frequency stability of a nonlinear MEMS oscillator under variable damping conditions. Analytical and experimental investigation of a MEMS square-wave oscillator embedding a double-ended tuning fork resonator driven into the non-linear regime is introduced. The experimental results indicate that for a pre-set drive level, the variation of air-damping changes the onset of nonlinear behaviour in the resonator, which not only impacts the output frequency but also the phase/frequency noise of a nonlinear MEMS square wave oscillator. The random walk frequency noise and flicker frequency noise levels are strongly correlated with the non-linear operating point of the resonator, whereas the white phase and white frequency noise levels are impacted both by the output power and by operative nonlinearities.**

***Index Terms*—MEMS, Oscillators, Nonlinear effects, Air Damping, Phase Noise.**

I. Introduction

SILICON microelectromechanical system (MEMS) resonator based oscillators are increasingly being adopted for various applications in timing and frequency control [1, 2] due to the reduced size, demonstrated compatibility with semiconductor batch manufacturing and integration with IC technologies. MEMS resonator based oscillators are also essential building blocks for resonant sensors [3-5]. One of the technical challenges limiting translation of resonant sensors has historically been reliability of the vacuum package though a number of technical solutions have been developed in recent years [6-8]. A second challenge relates to the susceptibility of MEMS resonators to non-linear effects limiting power handling resulting in the device often operated at the critical point or just prior to the onset of bifurcation in the response [9]. It is well established that the quality factor of a MEMS resonator typically limited by air damping at atmospheric pressure can be improved by operating the device in a vacuum ambient. This in turn brings potential benefits in terms of reduced power consumption and lowered noise floor [10, 11] when considering a linear noise model. On the other hand, the nonlinear threshold for MEMS resonators under harmonic force excitation, corresponding to bifurcation in the response, is predicted to onset at lower vibration amplitudes and corresponding lower power levels under vacuum environments, potentially limiting any gains in oscillator frequency instability obtained [12, 13]. However, an experimental investigation of these potentially competing effects has not been thoroughly investigated. A thorough understanding of these competing effects may also help inform optimal strategies for vacuum packaging resonator devices.

This paper investigates a MEMS square-wave (SW) oscillator[14] embedding a double-ended tuning fork (DETF) resonator in a feedback configuration. The DETF resonator has been previously employed for timing applications [15, 16] and resonant sensors [17-19]. The paper is organised as follows: in the following section, the SW oscillator topology is introduced. In section 3, analytical models are established to predict the linear and nonlinear behaviour of damped DETF resonators and the output frequency and frequency stability of the resulting SW oscillator under different damping conditions. Finally a prototype SW oscillator embedding a DETF MEMS resonator is implemented and experimentally characterized with results compared to analytical prediction.

II. MEMS Oscillator Topology

The topology of the MEMS oscillator studied in this paper is shown in Fig. 1. The oscillator consists of a micro-machined DETF resonator, a trans-impedance amplifier (TIA), an active band-pass filter, a comparator and a voltage divider. A parallel-plate electrostatic transduction mechanism is employed for excitation and detection of the motion of the DETF. The TIA amplifies and converts the motional current of the DETF resonator to a voltage signal which is fed to a band-pass filter whose output is supplied to the comparator. The DETF resonator is driven by a periodic voltage signal generated by the comparator of constant amplitude, pre-set by the voltage divider [14, 20].

Date submitted for review:
This work was supported in part by the Technology Strategy Board (Grant TP11/CAT/6/I/BP110G).
Xudong Zou is with the Nanoscience Centre, Department of Engineering, University of Cambridge. CB3 0FF United Kingdom (e-mail: xz280@cam.ac.uk).
Ashwin A. Seshia is with the Nanoscience Centre, Department of Engineering, University of Cambridge. CB3 0FF United Kingdom (e-mail: aas41@cam.ac.uk).

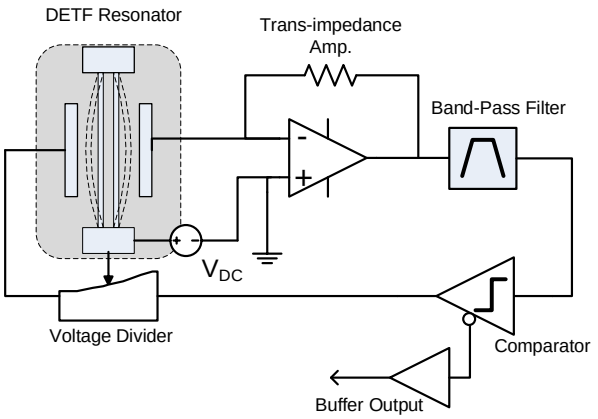

Fig. 1. Schematic of a MEMS square-wave oscillator embedding a micromachined DETF resonator.

III. Theoretical Analysis of a Damped Nonlinear Oscillator

A. Air Damping

The air damping associated with the DETF resonator is primarily expected to originate from the squeeze-film effect as the tuning fork tine vibrates towards the fixed electrode in a parallel-plate electrode configuration (see Fig. 2). Depending on the pressure level of the ambient in which the resonator is operated, either continuum or molecular models of gas damping have been previously proposed [21] . Qualitative determination of applicability of the appropriate model is indicated by the Knudsen number (*Kn*) [22], which is the ratio of the mean free path of the gas molecule (λ) to the characteristic length of the flow. The mean free path of air molecule can be calculated from (1), where k_B is the Boltzmann constant, T is the ambient temperature, σ is the cross-section area of air molecule and P is the pressure.

$$\lambda_{Air} = k_B T / \sqrt{2}\pi\sigma^2 P \tag{1}$$

The characteristic length of the flow in the DETF resonator is approximately equal to the gap between the two electrodes. As elaborated in future sections, the DETF resonator in this work is operated in a moderate vacuum ambient (< 5 torr). According to (1), the free path length of air molecule for pressure less than 5 torr is greater than 10 μm at room temperature, which is significantly larger than the gap size and makes the value of Kn typically >> 0.1. Therefore, the molecular approach is relevant to the air damping analysis in this scenario.

Several studies have been conducted on oscillating micro beams operated under low pressure conditions. The damping constant for resonators described in this paper are compared to the values predicted by Bao's energy transfer model [23] and Hutcherson's molecular dynamics model [21] which have been previously published with prior experimental validation at the MEMS-scale [24].

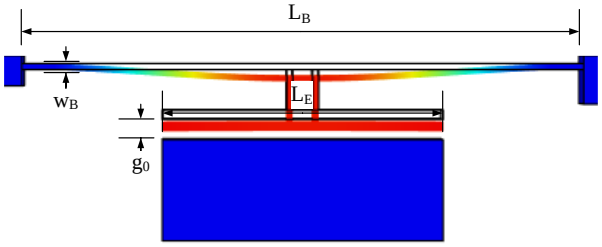

Fig. 2. Deformed geometry of one tine of the DETF resonator operating in the fundamental mode.

Since the DETF resonator is operated in the primary out-of-phase mode, the motion of the tines can be modelled similar to that of a clamped-clamped (CC) beam resonator due to mode symmetry. By applying the energy transfer model [23] to this CC beam resonator, the quality factor of the DETF can be estimated as:

$$Q_E = (2\pi)^{3/2} \frac{M_{eff}}{A_E} \left(\frac{g_0}{S}\right) \sqrt{\frac{RT}{M_m}} \frac{1}{P} \tag{2}$$

where $M_{eff} = \rho_{Si} t (0.375 L_B w_B + L_E w_E)$ (ρ_{si} is the density of silicon and t is the thickness of the device layer) is the effective mass of the resonator, $A_E = L_E \cdot t$ and $S = 2(L_E + t)$, are the area and perimeter of the electrode, g_0 is the gap between the two electrodes, R=*8.31 kg m²/(s²K)* is the universal molar gas constant, T is the temperature, M_m is the molar mass of the air and P is the ambient pressure. As previously outlined [21], a correction parameter, $C \approx 0.59$, is used as pre-multiplier to the right hand side of (2) to account for molecular collisions on the electrode surface. Equation 2 indicates that the quality factor Q for such a scenario is inversely proportional to the ambient pressure. If air damping dominates, the damping ratio of the DETF resonator, η, can then be correlated to the quality factor as:

$$\eta \approx \eta_{Air} = 1/2Q_E \tag{3}$$

B. Nonlinear MEMS Oscillator with Air Damping

A descriptive non-linear model for a MEMS square wave oscillator incorporating a non-linear tuning fork resonator has been previously developed [25]. In this section, this model is extended to consider the impact of air damping on oscillator performance.

1) Mechanical Nonlinearity

The resonator is often driven to large vibration amplitudes with a view towards optimizing the achievable signal-to-noise ratio. This view is accurate as long as the resonator is operated in the linear regime; however as the amplitude increases non-linear effects govern the response with significant deviations from the linear regime as the amplitude continues to increase. A comprehensive discussion of various operative nonlinearities in MEMS resonators can be found in several excellent references [26-28]. This paper primarily focuses on the influence of air damping on the geometrical nonlinearity associated with the vibration of clamped-clamped beams

(referred to as the 'amplitude-stiffening effect'), that primarily determines the non-linear response for these resonators.

For the DETF resonator operated in its fundamental in-plane flexural mode, the linear mechanical restoring force can be derived from classical beam theory:

$$F_k = k_{m1}x, k_{m1} = 16.23Et\left(\frac{w_B}{L_B}\right)^3 \tag{4}$$

where, k_{m1} is the linear mechanical spring constant, x is the transverse displacement of the resonator beam and E is the Young modulus of silicon. At higher vibration amplitudes, non-linearities in the restoring force arise due to the large beam deformation. This effect can be approximated by a cubic function of displacement being added to the restoring force defined by the spring constant, k_{m3}, as [25]:

$$F_{nk} = k_{m1}x + k_{m3}x^3 + O(x), k_{m3} = 0.751\frac{k_{m1}}{w_B^2} \tag{5}$$

As the DETF resonator is driven by an external harmonic force in the oscillator, the resonator response with nonlinear spring constant can be approximated as a lumped 1-DOF Duffing equation[25]:

$$M_{eff}\ddot{x} + 2\eta\sqrt{M_{eff}k_{m1}}\dot{x} + k_{m1}x + k_{m3}x^3 = F_{Act}\cos(\omega t) \tag{6}$$

where η is the linear damping ratio, $F_{Act}\cos(\omega t)$ is the external actuation force. An approximate solution to Eq.6 can be obtained by using perturbation analysis. The nonlinear amplitude-frequency, $x_{PN}(\omega)$, and phase-frequency, $\psi_N(\omega)$, responses of the DETF resonator can be determined as[13]:

$$x_{PN}(\omega) = \frac{F_{Act}}{2\omega_L M_{eff}\sqrt{(\eta\omega_L)^2 + \left(\omega - \omega_L - \frac{3k_{m3}x_{PN}^2}{8\omega_0 M_{eff}}\right)^2}} \tag{7}$$

$$\psi_N(\omega) = \tan^{-1}\frac{(\eta\omega_L)}{\left(\omega - \omega_L - \frac{3k_{m3}x_{PN}^2}{8\omega_0 M_{eff}}\right)} \tag{8}$$

where ω_L is the resonant frequency of DETF considering the linear spring term only.

Beyond a certain critical amplitude, the frequency response of the resonators starts to exhibit severe distortion from linear behaviour with the response curves kneeling over to the right describing multi-valued hysteretic behaviour. The critical bifurcation amplitude at which the resonator transitions from a single-valued to a multi-valued response can be related to the beam width (w_B) and the damping ratio[29] as:

$$x_c \approx C \cdot w_B\sqrt{2\eta} \tag{9}$$

Depending on the mode shape approximation used in the derivation, the coefficient, C, varies from 1.209[30] to 1.463[29]. Moreover, Equation 9 indicates that with increasing damping ratio, the critical amplitude also increases. This implies that for a given excitation force, a resonator operating in the nonlinear regime can be made linear by increasing the damping ratio.

2) Oscillation Criteria and Output Frequency

With reference to Fig. 1, the loop gain and phase conditions for the square wave oscillator can be expressed as:

$$G(\omega_{Opt}, x_p) = \frac{\varepsilon \cdot t \cdot L_E}{V_F \cdot g_0^2} V_{DC} \cdot \omega_{Opt} \cdot x_P \cdot R_{TIA} \geq 1 \tag{10}$$

$$\Psi(\omega_{Opt}, x_P) = \psi(\omega_{Opt}, x_P) + \varphi(\omega_{Opt}) + \phi_0 = 2n\pi, n = 0,1,2,... \tag{11}$$

where ε is the dielectric coefficient, L_E and t are the length and height of the parallel-plate electrode, g_0 is the gap between the two electrodes, V_F is the excitation voltage applied on the DETF, V_{DC} is the bias voltage applied on DETF, R_{TIA} is the gain of TIA, x_P is the vibration amplitude of DETF at oscillation, ω_{Opt} is the output angular frequency of the oscillator, ψ is the phase shift of DETF resonator, φ is the phase shift resulting from other circuit components and ϕ_0 is the phase shift contributed from other sources including electrical parasitics.

Although the DETF resonator may be operated in the nonlinear regime after stable oscillation is established, the linear model of DETF resonator can be still employed to analyze oscillation start-up criteria. Within the linear regime, the vibration amplitude and phase response of the beam of the DETF resonator at the resonant frequency can be estimated as:

$$x_{PL} = \frac{F'_{Act}}{\omega_r\sqrt{\eta^2 + \left(\omega_r M_{eff} - \frac{k_{m1}}{\omega_r}\right)^2}} \tag{12}$$

$$\psi_L = \tan^{-1}\left(\frac{\omega_r M_{eff} - \frac{k_{m1}}{\omega_r}}{\eta}\right) \tag{13}$$

$$\omega_r = \sqrt{\frac{k_{m1}}{M_{eff}} - 2\left(\frac{\eta}{2M_{eff}}\right)^2} \tag{14}$$

where ω_r is the linear angular resonant frequency of the DETF and F'_{Act} is the transient actuation force applied to the DETF resonator approximated by:

$$F'_{Act} \leq F_{Act} = \frac{\varepsilon \cdot t \cdot L_E}{g_0^2} V_{DC} \cdot V_{F0} \tag{15}$$

where V_{F0} is the set excitation voltage set by the comparator and voltage divider. Combining (10) – (15) we get:

$$G(\omega_r, x_{PL}) = \frac{\left(\frac{\varepsilon \cdot t \cdot L_E}{g_0^2} V_{DC}\right)^2}{\sqrt{\eta^2 + \left(\omega_r M_{eff} - \frac{k_{m1}}{\omega_r}\right)^2}} \cdot R_{TIA} > C_{st} > 1 \tag{16}$$

$$\Psi(\omega_r) = \tan^{-1}\left(\frac{\omega_r M_{eff} - \frac{k_{m1}}{\omega_r}}{\eta}\right) + \varphi(\omega_r) + \phi_0 = 2n\pi, n = 0,1,2... \tag{17}$$

where C_{st} is a non-dimensional number representing the gain margin for oscillator start-up, normally larger than 1 [31]. Equation 16 indicates that for a specific DETF resonator, the

increase of air damping will require a higher DC bias voltage (V_{DC}) and larger gain resistor to initiate oscillator start-up.

The growing oscillation amplitude is ultimately limited by a form of engineered non-linearity resulting in steady limit-cycle behaviour such that the excitation voltage applied to the DETF approaches the set value (V_{F0}). This set point may involve the resonator operating in the non-linear regime as shown in (6). However, there is always a unique solution of (6) associated with any initial condition[13]. As the dominant nonlinear spring constant is positive (i.e. the amplitude-stiffening nonlinearity) in this case, the angular frequency of the oscillator must increase to meet the oscillation criteria previously outlined. The output frequency of the nonlinear SW oscillator (f_{Opt}) can be derived by solving for the nonlinear response of the DETF resonator as shown in [25]:

$$f_{Opt} = \frac{\omega_{NL}}{2\pi} = \frac{1}{2\pi}\left[\omega_L + \frac{3}{8}\cdot\frac{k_{m3}}{\omega_L^3 M_{eff}}\cdot\left(\frac{V_{F0}}{2\eta\sqrt{k_{m1}M_{eff}}}\right)^2\cdot\left(\frac{\varepsilon\cdot t\cdot L_E}{g_0^2}V_{DC}\right)^2\right] \quad (18)$$

Equation 18 describes the output frequency of the nonlinear SW oscillator as a function of the damping ratio.

3) Phase/Frequency Noise

Phase/frequency noise[32] is a critical metric underlying oscillator frequency stability. For the nonlinear MEMS SW oscillator, phase/frequency noise may arise from the DETF resonator, the DC polarisation bias source, and the electronic components in the circuit. A discussion on the interaction of noise and non-linearity in MEMS oscillators has been previously discussed and predictive models to describe this interaction have been outlined[33, 34].

Mechanical-thermal noise in resonators has been previous studied [35-37] and there are two effects involved as the damping ratio is increased – 1) Quality factor is reduced, and 2) the onset of non-linearity appears at higher amplitudes limiting the role of noise up-mixing via non-linearity [38].

The noise in the DC polarization voltage of the resonator can also be converted to the phase/frequency noise of the SW oscillator in two ways. The first mechanism is mediated by transducer non-linearity. The 'electrostatic spring softening effect' can also translate DC polarization voltage noise into frequency fluctuations of the oscillator output [39] mediated through the 'amplitude-frequency' mixing effect when the resonator operated in the nonlinear regime. Since electrostatic spring softening is primarily determined by the design of parallel-plate electrodes and magnitude of the DC bias voltage, variation of the damping factor is not expected to significantly modulate this noise mechanism. However, the second noise conversion mechanism will be directly impacted by the variation of air damping of the DETF resonator as the amplitude-frequency nonlinear mixing effect is attenuated with increased damping.

The 'low frequency' component of amplitude noise injected by the electronics can also induce fluctuations in the excitation force that can be converted into frequency noise by the 'amplitude-frequency' mixing effect when the resonator is operated in the nonlinear regime. According to (7) and (18), increased damping will attenuate the 'amplitude-frequency' mixing effect as well as decreasing the vibration amplitude of the DETF resonator. As damping is increased, the 'linearized' DETF resonator will eliminate the phase/frequency noise arising due to the 'amplitude-frequency' mixing effect from the SW oscillator output signal. However, the reduced vibration amplitude of the DETF resonator will worsen the signal-to-noise ratio at the input of the TIA resulting in a degradation of the phase/frequency noise level.

IV. Experimental Results

A series of experiments were conducted to validate the theoretical analysis of the nonlinear SW oscillator under varying damping ratios. The geometrical dimensions of the DETF resonator employed is provided in Table 1. First, the response of the DETF resonator was measured open-loop in a pressure controlled vacuum chamber using a network analyser (Agilent 4396B) to extract the Q factors/damping ratios of the resonator under varying ambient pressure. Then, the open-loop amplitude/phase responses of DETF resonator under varying excitation voltage magnitudes and varying ambient pressures were tested. Finally, the DETF resonator was packaged and integrated together with the SW oscillator circuit on a PCB. The oscillator PCB was then inserted into a custom-designed pressure controllable vacuum chamber and the pressure in the chamber was gradually varied while simultaneously logging the output frequency of the oscillator using a frequency counter (Agilent 53230A).

TABLE I
Critical dimensions of the DETF resonator

DETF Beam Length (L_B)	360 μm
DETF Beam Width (w_B)	3.5 μm
Device Layer Thickness (t)	25 μm
Electrode Length (L_E)	177 μm
Electrode Width (w_E)	7.5 μm
Gap between Electrodes (g_0)	3 μm

A. Q Factor of DETF Resonator

Fig. 3 plots the experimentally measured Q factors of the DETF resonator under varying ambient pressure at room temperature. The predicted Q-factors as dictated by the two analytical models introduced in section 3.A are plotted as well.

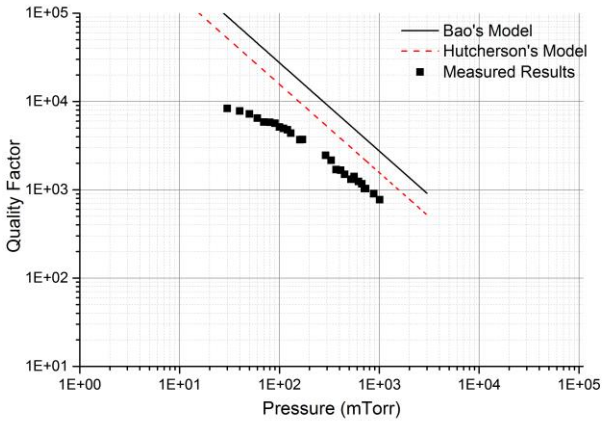

Fig. 3. Measured Quality factor of the DETF resonator under varying ambient pressure.

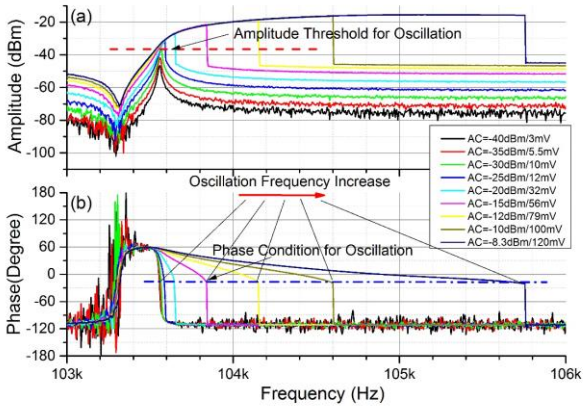

Fig. 4. Measured open-loop amplitude (a) and phase (b) frequency response of the DETF resonator with varying excitation voltage magnitude at a pressure level of 30 mtorr.

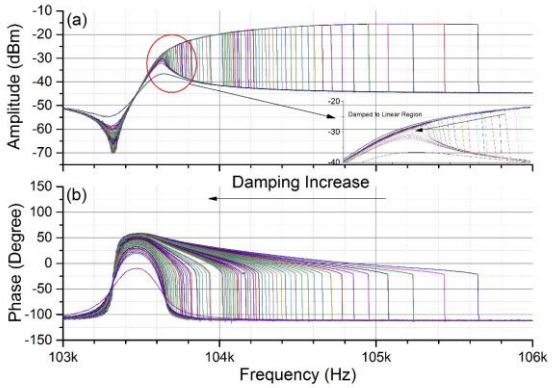

Fig. 5. Measured amplitude (a) and phase (b) frequency response of the DETF resonator with varying damping ratios.

An independent pressure gauge was used to record the ambient pressure in the chamber which was varied from 30 mTorr to 1 Torr. As seen in Fig. 3, the measured quality factor of DETF resonator (square dots) decreases with the increasing pressure, in agreement with the trend predicted by the analytical models. This result indicates that the quality factor/damping ratio of this DETF resonator is dominated by air damping when the ambient pressure is greater than 40 mTorr. Also, the measured Q value is lower than that predicted by analytical models, indicating other operative energy loss mechanisms, not sensitive to the ambient pressure limiting Q at lower ambient pressure levels, such as anchor loss[40] and thermo-elastic damping.

B. Nonlinear Response of DETF Resonator

In order to validate the analysis presented in section III.B, two stepped parametric open-loop characterization experiments were performed on the resonator in a customized vacuum chamber. For the first set of measurements, the pressure level inside the vacuum chamber was set at 30 mTorr and the amplitude and phase frequency response of the resonator is measured while the excitation voltage applied is gradually increased from 3mV to 120mV (See Fig. 4). In the second set of measurements, the excitation voltage on the DETF resonator was fixed at 120mV and the amplitude and phase responses of DETF resonator were measured with the ambient pressure in the chamber gradually increased from 40m Torr to 3 Torr (See Fig. 5). Since the DETF resonator was operated at a vibration amplitude that is significantly smaller than a third of transduction gap, the measured output current/voltage is proportional to the vibration amplitude (x_P) of the DETF beams[25] and the non-linearity of the transducer is significantly smaller.

As shown in Fig. 4, with increasing excitation voltage magnitudes, the frequency response of the DETF resonator moves from the linear regime (described by (12) and (13)) to the nonlinear regime (described by (7) and (8)). For this particular DETF resonator, the linear threshold excitation voltage magnitude is about 10mV when Q equals approximately 9,000. Small signal excitation conditions may be assumed at oscillation start-up and hence the amplitude/phase responses of DETF resonator can be assumed to be linear to analyse start-up conditions. Assuming the oscillation criteria (described by (11)) are satisfied, the output signal of the oscillator grows until the amplitude is limited by specific non-linearity for e.g. by an automatic amplitude control mechanism built into the circuit (in this case limiting the amplitude to a value pre-set by the comparator and voltage divider in the oscillator circuit). Fig. 4 shows that the non-linear phase frequency response will dictate the operating point for the oscillator as the amplitude criterion is always satisfied within the feedback loop.

Increasing the damping ratio results in the onset of non-linearity at higher excitation voltages as shown in the previous section and this is also consistent with the experimental results shown in Fig. 5. As the ambient pressure in the vacuum chamber increases, increased air damping results in reduced nonlinear behaviour of the DETF resonator for the

same excitation voltage conditions and the resonator can be operated in the linear regime at sufficiently high damping levels (as shown in the plot in Fig. 5). However, it should be noted that increase in air damping will also increase the motional resistance of the DETF resonator ultimately resulting in the oscillation criteria not being met.

C. Resonant Frequency Variation with Air Damping

The DETF resonator and electronic circuit components are integrated on a single PCB to implement the SW oscillator. The DC polarization voltage applied on the resonator is 10 V and the feedback excitation voltage is set to 120 mV. The oscillator board is placed inside the pressure controllable vacuum chamber as before and the output frequency of the oscillator is recorded using an Agilent 53230A frequency counter.

Fig. 6 plots the measured output frequency of the SW oscillator under varying resonator damping ratios with a comparison provided with respect to the analytical model (18). It is seen that the measured output frequencies matches well with the analytical model. Additionally, it was noted that the SW oscillator stopped working when ambient pressure increased to about 3 Torr, corresponding to a damping ratio of 1E-3.

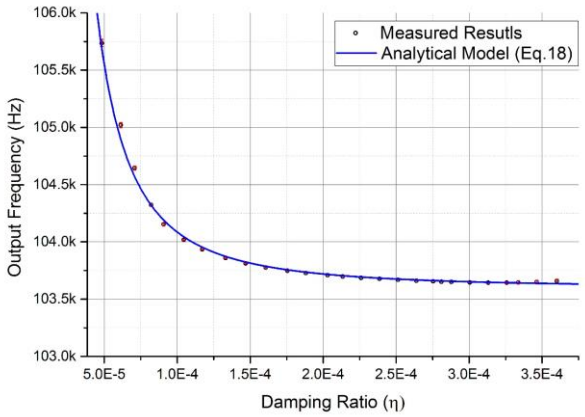

Fig. 6. Plot of the output frequency of the SW oscillator with varying damping ratios of the DETF resonator.

D. Allan Variance with Variable Air Damping

In order to investigate the influence of air damping on oscillator noise, the Allan Variance (σ_y^2)[41] was calculated for a series of oscillator frequency measurements with different damping ratios (see Fig. 7). For the Allan Variance/Deviation plot, various noise mechanisms underlying the measured response can be distinguished by the different slopes on the graph[32]. As seen in Fig. 7, the measured frequency stability of the nonlinear SW oscillator exhibits strong dependence on the damping ratio of the DETF resonator (limited by air damping for these measurements). When the air damping is relatively low, the oscillator output frequency stability is seen to be relatively poor with evidence for at least four noise mechanisms (η=4.8E−5). With increasing level of air damping (η=5.8E−5~8.9E−5), the random walk frequency noise level decayed rapidly and the flicker frequency noise level also reduced. However, the white phase noise and white frequency noise level is not significantly impacted at this stage. When the air damping is further increased (η=1.2E−4~2.9E−4), the flicker frequency noise level is seen to reduce and the random walk frequency noise process is not observed for averaging times up to 10s. The white phase and white frequency noise levels are also seen to reduce. However, when air damping is further increased (η>3E−4), the white phase and white frequency noise levels are significantly increased with no corresponding increase in the levels of the random walk frequency and flicker frequency noise levels. The minimum fractional frequency deviation of the square wave oscillator is approximately 25 ppb for an 8 second averaging time when the damping ratio is about 2.8E-4, which is approximately 15 times smaller than for the case of the same oscillator operating at low pressure when the damping ratio is about 4.8E-5.

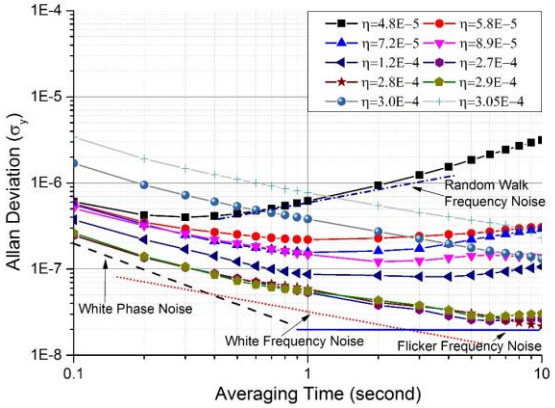

Fig. 7. Allan Deviation of the SW oscillator output signal with different resonator damping ratios.

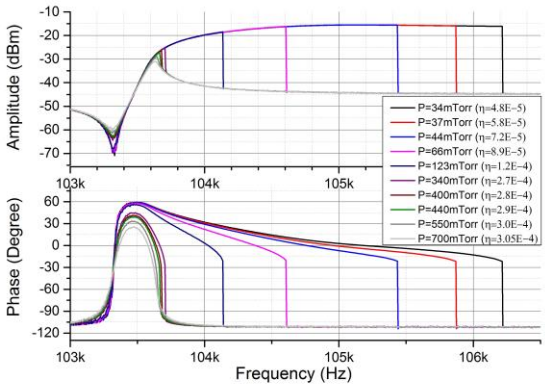

Fig. 8. Measured open-loop amplitude and phase frequency response of the DETF resonator with resonator damping ratios corresponding to the measured Allan Deviation results shown in Fig. 7.

According to (7)-(9) and the open-loop measurement results shown in Fig. 8, an increase in the damping factor will allow for operation at higher elevated amplitudes. In the meantime, the random walk frequency and flicker frequency noise levels in the square-wave oscillator are also significantly reduced, indicating that these two noise components appear to strongly correlate with resonator nonlinearity due to the nonlinear amplitude-frequency mixing effect. The white phase and white frequency noise regimes in the SW oscillator exhibit a

dependence on the damping factor as well. The increase of air-damping does not significantly influence the white phase and white frequency noise level of the SW oscillator until the resonator starts to transition from the critical nonlinear regime to the linear regime with increasing air-damping. However, upon further increase in air-damping in the linear regime, the white phase and white frequency noise components show a significant increase over and beyond what is observed when the DETF resonator operated in nonlinear regime. The increase in this noise level is due to the reduced vibration amplitude of the tines corresponding to a reduced output power and reduced quality factor.

In summary, the experimental results show that the random walk frequency noise and flicker frequency noise level are strongly related to the non-linearity of the DETF resonator, whereas the white phase and white frequency noise levels are impacted both by the output power and by resonator non-linearity. Therefore, there exists an optimal damping level for a particular SW oscillator coinciding with the transition between the linear and nonlinear regimes to optimize the frequency stability of the oscillator. In practice, the excitation voltage amplitude produced by the oscillator circuit should set the resonator operating point just at the onset of the nonlinear regime and not well into the regime described by hysteresis in the frequency response or well within the regime described by a linear model for best results. Further, the experimental results indicate that the design regime for optimized frequency stability is not necessarily restricted to a single operating point; however, further detailed investigation will be necessary to investigate the degree of sensitivity to small changes to device parameters and ambient conditions about the optimal operating regime.

V. Conclusion

This paper investigates the impact of air-damping on the output frequency and phase/frequency stability of a nonlinear MEMS square wave oscillator. Analytical models are constructed for the air-damped nonlinear DETF resonator and the square wave oscillator to provide physical insight into the prediction of the influence of damping on oscillator performance. The analysis and predictions are then examined and validated by a series of carefully designed laboratory tests. Both theoretical and experimental studies indicate that when air-damping dominates the damping ratio of the DETF resonator, the increase of pressure will impact the output frequency of the nonlinear square-wave oscillator. The variation of the damping ratio also influences the phase/frequency noise of the square-wave oscillator. For a particular design of the DETF resonator and specified circuit parameters, an optimal air-damping/pressure level exists for the case of optimal frequency stability. This finding indicates that the DETF resonator or other similar resonators used for the SW oscillator topology may not require very low pressure levels to achieve optimal frequency stability since the noise floor of the oscillator may increase in low damping conditions due to the onset of significant nonlinearities.

References

[1] W. T. Hsu, Recent progress in silicon MEMS oscillators, 40th Annual Precise Time and Time Interval Meeting, Reston, VA, Dec. 2008..

[2] C.T-C. Nguyen, "MEMS technology for timing and frequency control," *Ultrasonics, Ferroelectrics and Frequency Control, IEEE Transactions on*, vol. 54, pp. 251-270, 2007.

[3] A. A. Seshia, M. Palaniapan, T. A. Roessig, R. T. Howe, R. W. Gooch, T. R. Schimert, *et al.*, "A vacuum packaged surface micromachined resonant accelerometer," *Journal of Microelectromechanical Systems*, vol. 11, pp. 784-793, 2002.

[4] S. S. Bedair and G. K. Fedder, "CMOS MEMS oscillator for gas chemical detection," in *Sensors, 2004. Proceedings of IEEE*, 2004, pp. 955-958.

[5] X. Zou, P. Thiruvenkatanathan, and A. Seshia, "Micro-electro-mechanical resonant tilt sensor," in *Frequency Control Symposium (FCS), 2012 IEEE International*, 2012, pp. 1-4.

[6] V. Kaajakari, J. Kiihamäki, A. Oja, S. Pietikäinen, V. Kokkala, and H. Kuisma, "Stability of wafer level vacuum encapsulated single-crystal silicon resonators," *Sensors and Actuators A: Physical*, vol. 130, pp. 42-47, 2006.

[7] R. W. Gooch, Vacuum package fabrication of microelectromechanical system devices with integrated circuit components: U.S. Patent 6,479,320[P]. 2002-11-12..

[8] R. N. Candler, M. A. Hopcroft, B. Kim, W.-T. Park, R. Melamud, M. Agarwal, *et al.*, "Long-term and accelerated life testing of a novel single-wafer vacuum encapsulation for MEMS resonators," *Microelectromechanical Systems, Journal of*, vol. 15, pp. 1446-1456, 2006.

[9] V. Kaajakari, T. Mattila, A. Oja, and H. Seppa, "Nonlinear limits for single-crystal silicon microresonators," *Microelectromechanical Systems, Journal of*, vol. 13, pp. 715-724, 2004.

[10] V. Kaajakari, T. Mattila, A. Oja, J. Kiihamaki, H. Kattelus, M. Koskenvuori, *et al.*, "Square-extensional mode single-crystal silicon micromechanical RF-resonator," in *TRANSDUCERS, Solid-State Sensors, Actuators and Microsystems, 12th International Conference on, 2003*, 2003, pp. 951-954.

[11] J. E-Y. Lee, Y. Zhu, and A. Seshia, "A bulk acoustic mode single-crystal silicon microresonator with a high-quality factor," *Journal of micromechanics and microengineering*, vol. 18, p. 064001, 2008.

[12] M. Agarwal, P. Kwan-Kyu, R. N. Candler, K. Bongsang, M. A. Hopcroft, S. A. Chandorkar, *et al.*, "Nonlinear Characterization of Electrostatic MEMS Resonators," in *International Frequency Control Symposium and Exposition, 2006 IEEE*, 2006, pp. 209-212.

[13] I. Kovacic and M. J. Brennan, The Duffing equation: nonlinear oscillators and their behaviour: John Wiley & Sons, 2011.

[14] J.E-Y. Lee, B. Bahreyni, Y. Zhu, and A. A. Seshia, "A single-crystal-silicon bulk-acoustic-mode microresonator oscillator," *Electron Device Letters, IEEE*, vol. 29, pp. 701-703, 2008.

[15] J. Van Beek and R. Puers, "A review of MEMS oscillators for frequency reference and timing applications," *Journal of Micromechanics and Microengineering*, vol. 22, p. 013001, 2012.

[16] S. M. Kashmiri and K. A. Makinwa, "Silicon-Based Frequency References," in *Electrothermal Frequency References in Standard CMOS*, ed: Springer, 2013, pp. 15-44.

[17] T.-A. W. Roessig, "Integrated MEMS tuning fork oscillators for sensor applications," University of California, Berkeley, 1998.

[18] R. G. Azevedo, D. G. Jones, A. V. Jog, B. Jamshidi, D. R. Myers, C. Li, *et al.*, "A SiC MEMS Resonant Strain Sensor for Harsh Environment Applications," *Sensors Journal, IEEE*, vol. 7, pp. 568-576, 2007.

[19] M. S. Weinberg and A. Kourepenis, "Error sources in in-plane silicon tuning-fork MEMS gyroscopes," *Microelectromechanical Systems, Journal of*, vol. 15, pp. 479-491, 2006.

[20] K. E. Wojciechowski, "Electronics for resonant sensors," PhD thesis, University of California, Berkeley, 2005.

[21] H. Sumali, "Squeeze-film damping in the free molecular regime: model validation and measurement on a MEMS," *Journal of Micromechanics and Microengineering*, vol. 17, p. 2231, 2007.

[22] C.-M. Ho and Y.-C. Tai, "Micro-electro-mechanical-systems (MEMS) and fluid flows," *Annual Review of Fluid Mechanics*, vol. 30, pp. 579-612, 1998.

[23] M. Bao and H. Yang, "Squeeze film air damping in MEMS," *Sensors and Actuators A: Physical*, vol. 136, pp. 3-27, 2007.

[24] J. Zook, D. Burns, H. Guckel, J. Sniegowski, R. Engelstad, and Z. Feng, "Characteristics of polysilicon resonant microbeams," *Sensors and Actuators A: Physical*, vol. 35, pp. 51-59, 1992.

[25] D. K. Agrawal, J. Woodhouse, and A. A. Seshia, "Modeling nonlinearities in MEMS oscillators," *Ultrasonics, Ferroelectrics and Frequency Control, IEEE Transactions on*, vol. 60, 2013.
[26] M. Younis and A. Nayfeh, "A study of the nonlinear response of a resonant microbeam to an electric actuation," *Nonlinear Dynamics*, vol. 31, pp. 91-117, 2003.
[27] V. Kaajakari, T. Mattila, A. Lipsanen, and A. Oja, "Nonlinear mechanical effects in silicon longitudinal mode beam resonators," *Sensors and Actuators A: Physical*, vol. 120, pp. 64-70, 2005.
[28] I. Kozinsky, H. C. Postma, I. Bargatin, and M. Roukes, "Tuning nonlinearity, dynamic range, and frequency of nanomechanical resonators," *Applied Physics Letters*, vol. 88, p. 253101, 2006.
[29] J. Juillard, A. Bonnoit, E. Avignon, S. Hentz, N. Kacem, and E. Colinet, "From MEMS to NEMS: closed-loop actuation of resonant beams beyond the critical Duffing amplitude," in *Sensors, 2008 IEEE*, 2008, pp. 510-513.
[30] L. Nicu and C. Bergaud, "Modeling of a tuning fork biosensor based on the excitation of one particular resonance mode," *Journal of Micromechanics and Microengineering*, vol. 14, p. 727, 2004.
[31] F. He, R. Ribas, C. Lahuec, and M. Jézéquel, "Discussion on the general oscillation startup condition and the Barkhausen criterion," *Analog Integrated Circuits and Signal Processing*, vol. 59, pp. 215-221, 2009.
[32] E. Rubiola, *Phase noise and frequency stability in oscillators*. Cambridge, UK ; New York: Cambridge University Press, 2009.
[33] T. A. Roessig, R. T. Howe, and A. P. Pisano, "Nonlinear mixing in surface-micromachined tuning fork oscillators," in *Frequency Control Symposium, 1997., Proceedings of the 1997 IEEE International*, 1997, pp. 778-782.
[34] B. Yurke, D. Greywall, A. Pargellis, and P. Busch, "Theory of amplifier-noise evasion in an oscillator employing a nonlinear resonator," *Physical Review A*, vol. 51, p. 4211, 1995.
[35] A. N. Cleland and M. L. Roukes, "Noise processes in nanomechanical resonators," *Journal of Applied Physics*, vol. 92, pp. 2758-2769, 2002.
[36] J. R. Vig and Y. Kim, "Noise in microelectromechanical system resonators," *Ieee Transactions on Ultrasonics Ferroelectrics and Frequency Control*, vol. 46, pp. 1558-1565, 1999.
[37] Z. Djuric, "Mechanisms of noise sources in microelectromechanical systems," *Microelectronics Reliability*, vol. 40, pp. 919-932, 2000.
[38] V. Kaajakari, J. K. Koskinen, and T. Mattila, "Phase noise in capacitively coupled micromechanical oscillators," *Ultrasonics, Ferroelectrics and Frequency Control, IEEE Transactions on*, vol. 52, pp. 2322-2331, 2005.
[39] X. Zou, P. Thiruvenkatanathan, and A. A. Seshia, "Micro-electro-mechanical resonant tilt sensor with 250 nano-radian resolution," in *European Frequency and Time Forum & International Frequency Control Symposium (EFTF/IFC), 2013 Joint*, 2013, pp. 54-57.
[40] J.E-Y. Lee, J. Yan, and A. A. Seshia, "Anchor limited Q in flexural mode resonators," in *Ultrasonics Symposium, 2008. IUS 2008. IEEE*, 2008, pp. 2213-2216.
[41] D. W. Allan, "Statistics of atomic frequency standards," *Proceedings of the Institute of Electrical and Electronics Engineers*, vol. 54, pp. 221-&, 1966.